



Microstructure evolution of the $\text{Si}_3\text{N}_4/\text{Si}_3\text{N}_4$ joints brazed using Au–Ni–V filler alloys with different V content

Y. Sun, J. Zhang*, H.W. Zhang, G.H. Fan, Y.M. He

School of Materials Science and Engineering, Harbin Institute of Technology, Harbin 150001, China

ARTICLE INFO

Article history:

Received 14 January 2011

Received in revised form 24 May 2011

Accepted 28 May 2011

Available online 6 June 2011

Keywords:

Silicon nitride

Brazing

Interfaces

Microstructure

Au–Ni–V filler alloy

ABSTRACT

Au–Ni–V filler alloys with different vanadium contents were designed to braze Si_3N_4 ceramic at 1373 K for 30 min, and the microstructures of brazing seams were investigated by SEM and TEM. When the Au–Ni–V filler alloy contains 5 at.% V, round-like $\text{Ni}[\text{Si}, \text{V}, \text{Au}]$ precipitates form in the $\text{Au}[\text{Ni}]$ solid solution matrix and a VN reaction layer with 0.5 μm thickness appears on Si_3N_4 interface. When the V content increases to 10 at.%, a new polygonal Ni_2SiV_3 phase occurs in the seam, and the $\text{Ni}[\text{Si}, \text{V}, \text{Au}]$ precipitate coarsens and VN layer thickens. With increase of V contents to 15 and 20 at.%, laminar $\text{Ni}[\text{Au}]$ and polygonal Ni_3V precipitates form. With 25 at.% V content in the filler alloy, the Ni_2SiV_3 and Ni_3V precipitates distribute homogeneously in the brazing seam. These microstructure evolutions were attributed to the reaction between Si_3N_4 and vanadium, which forms VN reaction layer and releases Si into the molten alloy.

© 2011 Elsevier B.V. All rights reserved.

1. Introduction

Nitride ceramic, especially Si_3N_4 , is the most attractive engineering ceramic for high-temperature application due to their excellent mechanical properties, resistance to corrosive environments and creep resistance at high temperature [1,2]. The strong covalent bonding between Si and N contributes to their attractive properties. However, the strong bonding also makes Si_3N_4 ceramic difficult to manufacture large-size or complex shape ceramic components [3]. Therefore, the joining of ceramics was investigated widely.

During recent years, various methods have been developed to join Si_3N_4 ceramic, involving active metal brazing [4,5], solid state diffusion bonding [6,7], partial transient liquid phase bonding [8,9], glass–ceramics bonding and so on [10,11]. Of all the joining techniques, active metal brazing is an attractive technique for industrial applications due to its simplicity, small capital investment and perfect adaptability of size and shape of joint.

Most of the investigations in brazing Si_3N_4 ceramics have focused on active brazing alloys with the active element Ti in last two decades. The results have shown that Ti element is characterized as having sufficient thermodynamic driving force to destabilize the covalent bonding of Si_3N_4 ceramic by reacting with N and Si,

leading to the formation of TiN and Ti_5Si_3 reaction layers. The reliable joints can be obtained by the strong interfacial bonding [12,13]. Generally, most of the current researches concerning the Ti-activated filler alloys focused on the following aspects: (1) the exploration of elements and composition ratio of active brazing alloys for brazing ceramics; (2) the effect of brazing parameters on the microstructure and mechanical properties of the joints; (3) the examination of the reaction products and behavior of the interfacial reaction [14–17]. The bonding mechanism of the Ti-activated filler alloy has been studied deeply and systematically. However, the metals in Group IV and V, such as Hf, Zr, and V, also can add into the filler metal as active elements, by which reaction products and mechanism of the interfacial reaction have not been reported systematically [18–20].

In recent year, it is of critical importance to develop active brazing alloys with high melting point and oxidation-resistance in order to satisfy the application of ceramic joint at high temperature. Therefore, the active V element was paid more and more attention due to its superior high-temperature oxidation resistance. Some researches have reported that the active V element can react with Si_3N_4 to form nitrogen vanadium compounds, so a high quality interfacial bonding could be obtained [21–24]. According to literatures [23,24], the $\text{Si}_3\text{N}_4/\text{Si}_3\text{N}_4$ joints brazed with Au–Ni–V and Au–Ni–V–Mo filler alloys not only have reliable room temperature strength, but also present excellent high temperature performance. Unfortunately, few researches concerning the effect of vanadium content in the filler alloys on the microstructure of the $\text{Si}_3\text{N}_4/\text{Si}_3\text{N}_4$ joint were reported up to now. In this paper, Au–Ni–V filler alloys

* Corresponding author.

E-mail address: hitzhangjie@hit.edu.cn (J. Zhang).

with different V content were used to join Si_3N_4 ceramics, and microstructure evolution was investigated deeply.

2. Materials and experimental procedures

In the experiment, the Si_3N_4 ceramic was sintered by the hot-pressing process (Institute of ceramics, Shanghai, China). A small amount of Al_2O_3 and Y_2O_3 were used as sintering additives. The pre-prepared process of Si_3N_4 samples was reported early in the literature [24]. The filler alloys are pure Au, Ni and V metal foils with thickness of 20 μm for each. Five kinds of filler alloys were obtained by weighing the three kinds of metal foil, having the same Au:Ni ratio but different V content (Table 1).

After the ceramics and filler alloys were prepared and fixed by cyanacrylate adhesives as the literature [25], the specimen assembly was put into a vacuum furnace and a uniaxial pressure of 1.63 kPa perpendicular to the bonding interfaces was

Table 1
Composition of the brazing filler alloys.

Designation	Composition (at.%)		
	Au	Ni	V
V5	56.1	38.9	5
V10	53.1	36.9	10
V15	50.2	34.8	15
V20	32.8	47.2	20
V25	30.7	44.3	25

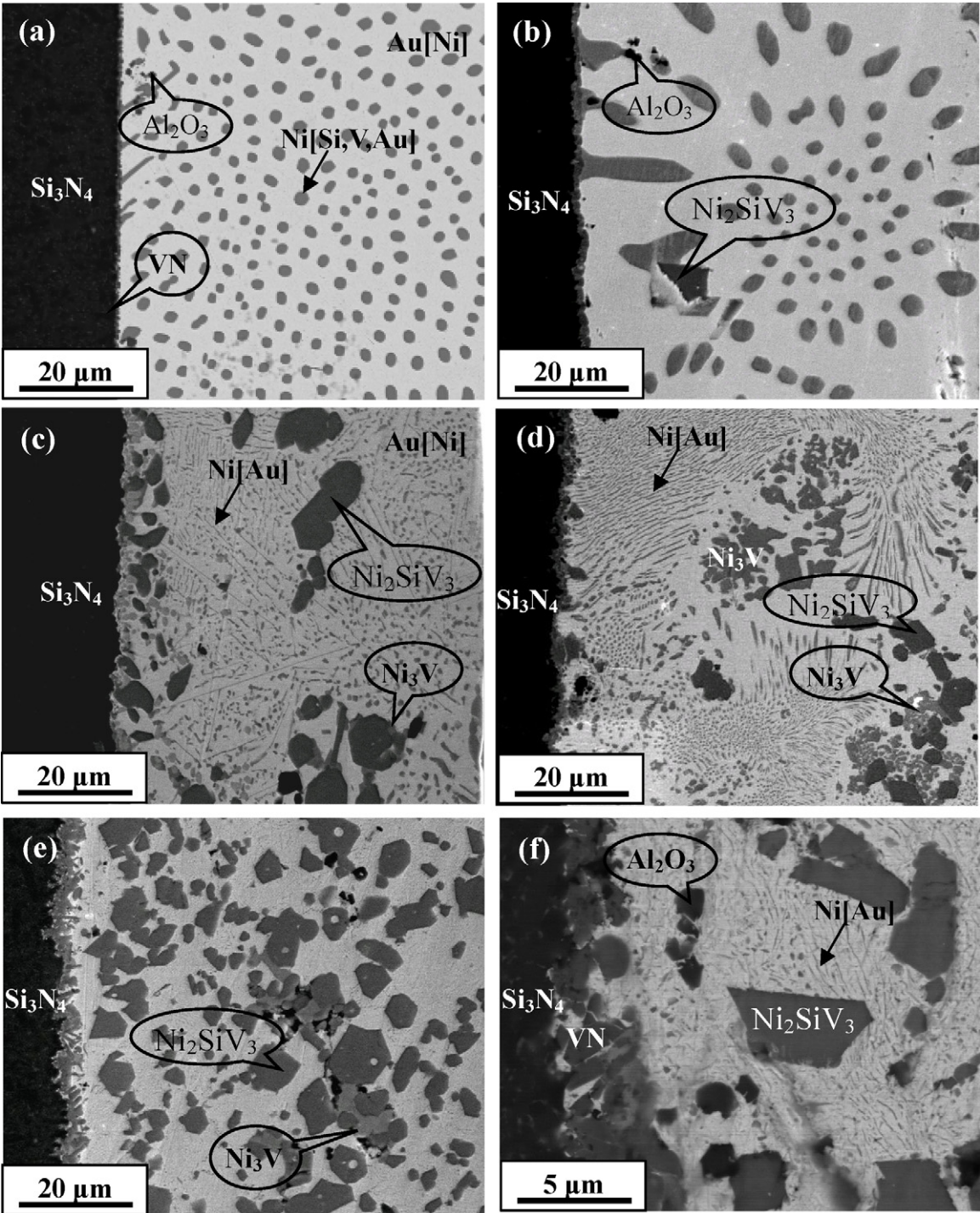


Fig. 1. SEM images of the $\text{Si}_3\text{N}_4/\text{Si}_3\text{N}_4$ ceramic joints brazed by Au–Ni–V filler alloys with different V content: (a) V5; (b) V10; (c) V15; (d) V20; (e) and (f) V25.

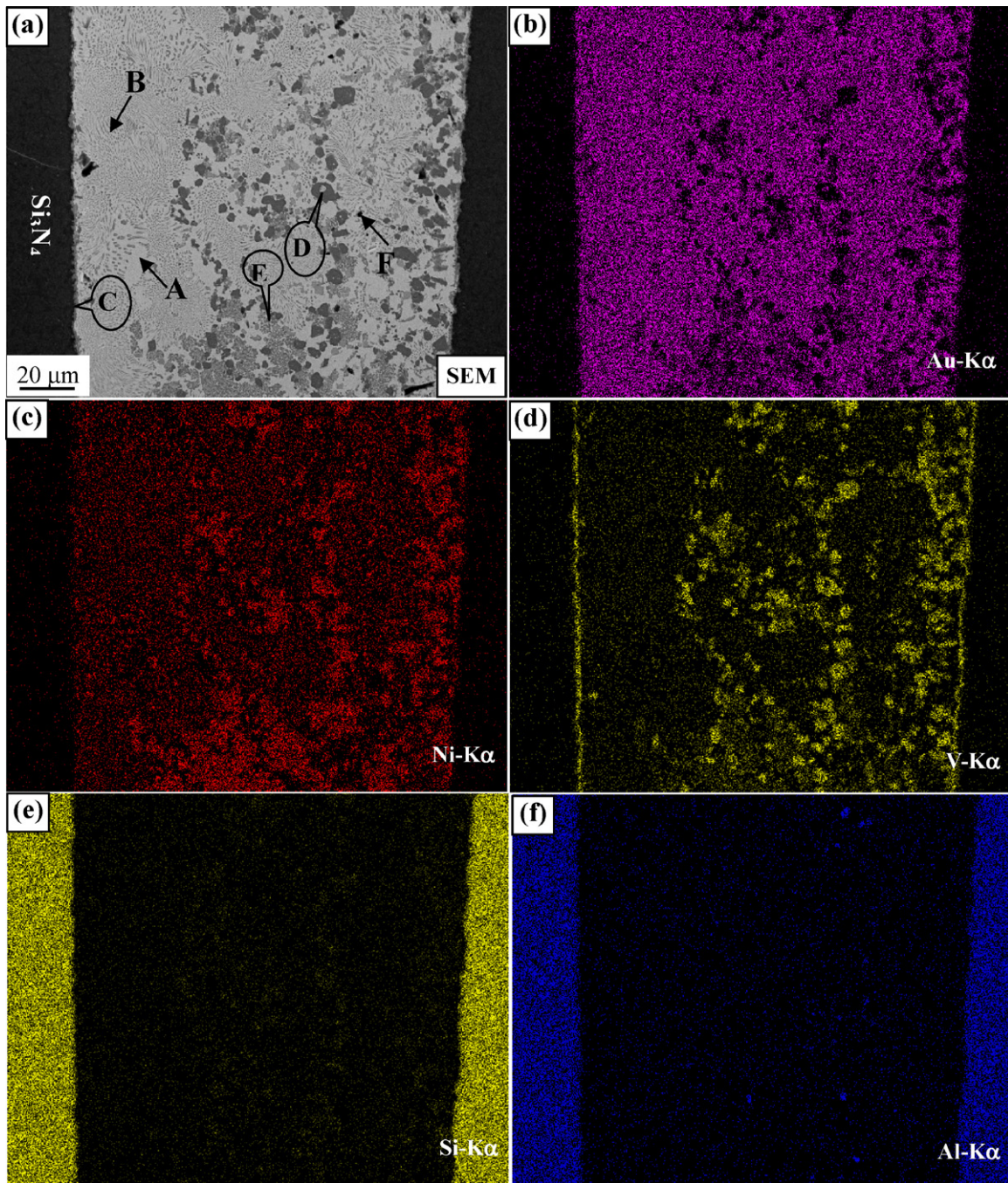


Fig. 2. (a–f) SEM image and elemental analysis of joint brazed by using V20 filler alloy.

applied to the specimen to keep them contact tightly. The vacuum in the furnace was kept in the range of 1.0×10^{-3} to 3.0×10^{-3} Pa.

During brazing, the specimens were firstly heated to 573 K at a rate of 20 K/min, and held for 20 min to make cyanacrylate adhesives volatilize and ensure the brazing surfaces clean. Then, the specimens were heated to 1373 K at a rate of 5 K/min and held for 30 min at the brazing temperature. At last, the specimens were cooled down to 573 K at 5 K/min, and then cooled in furnace without power.

The microstructure of the joints was investigated and analyzed by scanning electron microscopy (SEM) coupled with energy dispersive spectroscopy (EDS). The reaction phases in the joint were identified by transmission electron microscopy (TEM). The TEM specimen with the thickness of 0.2 μm was fabricated by Focused ion beam (FIB) technique.

3. Results

Fig. 1 shows SEM micrographs of the $\text{Si}_3\text{N}_4/\text{Si}_3\text{N}_4$ ceramic joints brazed at 1373 K for 30 min by Au–Ni–V filler alloys with differ-

ent V content. In the figure, the dark region on the left is Si_3N_4 ceramic. A reaction layer VN is observed near Si_3N_4 ceramic, which exhibits sound interfacial bonding without any defects. The bright region on the right is the filler, which consists of several phases, such as the matrix of Au[Ni] solid solution, Ni-rich phase precipitates and some reactant phases. From Fig. 1(a)–(e), it can be found that with increasing V content in Au–Ni–V filler alloy the reaction layer thickens, and more reactant phases occur in the center of the brazing seam.

Fig. 1(a) shows microstructure of the joint brazed with V5 filler alloy. According to our previous researches [24,25], the brazing seam consists of Au[Ni] solid solution as matrix alloy, the Ni[Si, V, Au] solid solution including 8.7 at.% Si and 6.7 at.% V, and the continuous and compact reaction layer VN with thickness of 0.5 μm between Si_3N_4 ceramic and the filler.

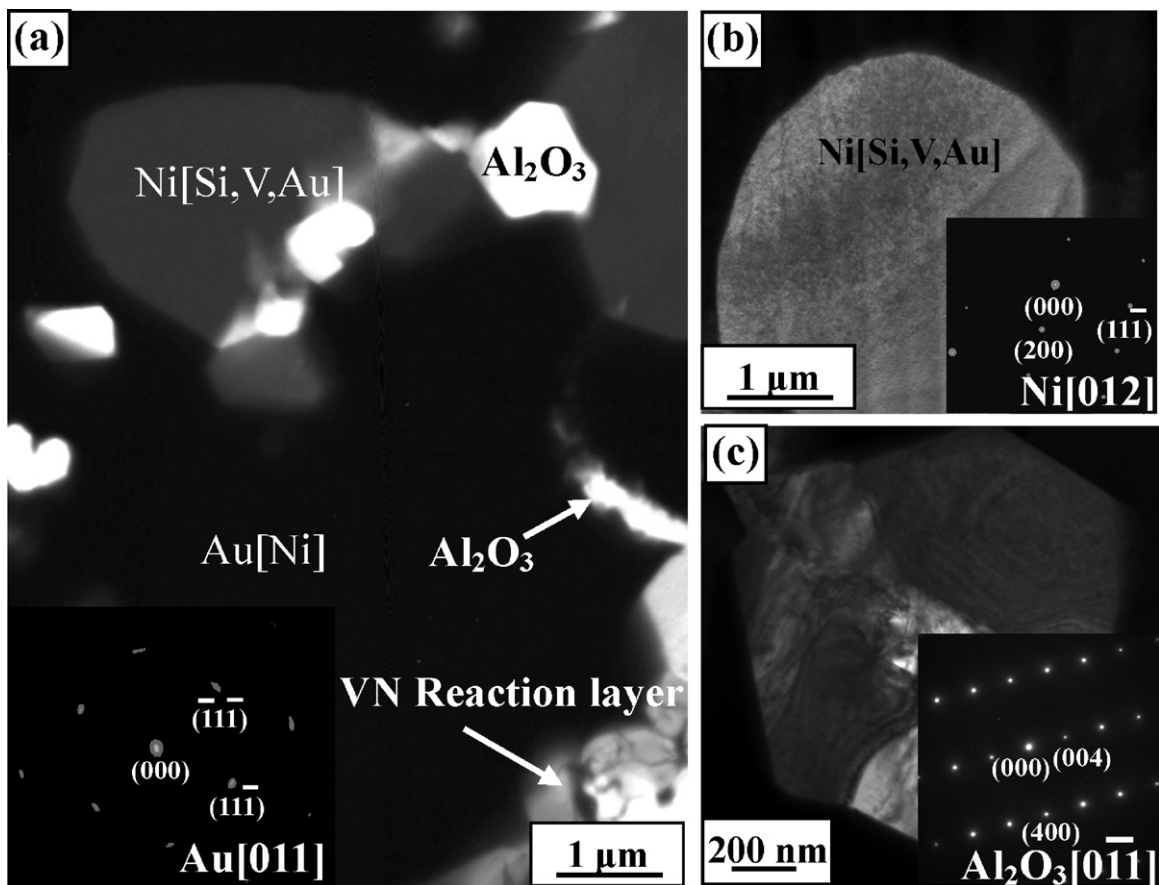


Fig. 3. TEM results of the joint brazed by V10 filler alloy: (a) the brazing seam (b) Ni[Si, V, Au] solid solution, (c) Al₂O₃ ceramic particle.

As shown in Fig. 1(b), it can be seen that the thickness of reaction layer reaches to 1 μm when the V10 filler alloy was used to join Si₃N₄ ceramic. Besides Au[Ni] and Ni[Si, V, Au] solid solution, a gray polygonal phase occurs in brazing seam. According to EDS result, its composition is Ni_{32.4}Si_{17.1}V_{50.5} (at.%), which implies that the ternary phase may be Ni₂SiV₃. The result agrees with isothermal cross-section of Ni–Si–V phase diagram [26] at 1373 K and will be testified by TEM later. Moreover, some black particles are detected in brazing seam and near the VN reaction layer, which were com-

posed of Al and O with composition of Al_{38.2}O_{61.8} (at.%). It is identified as Al₂O₃ ceramic particles.

With further increase of V content to 15 and 25 at.%, the thickness of reaction layer at the Si₃N₄ ceramic/the filler and the amount of Ni₂SiV₃ phases in the joint increase obviously. Moreover, a new phase occurs in the joint. As shown in Fig. 1(c) and (d), it also can be found that round-like Ni[Si, V, Au] solid solution phase changes to the laminar Ni[Au] solid solution.

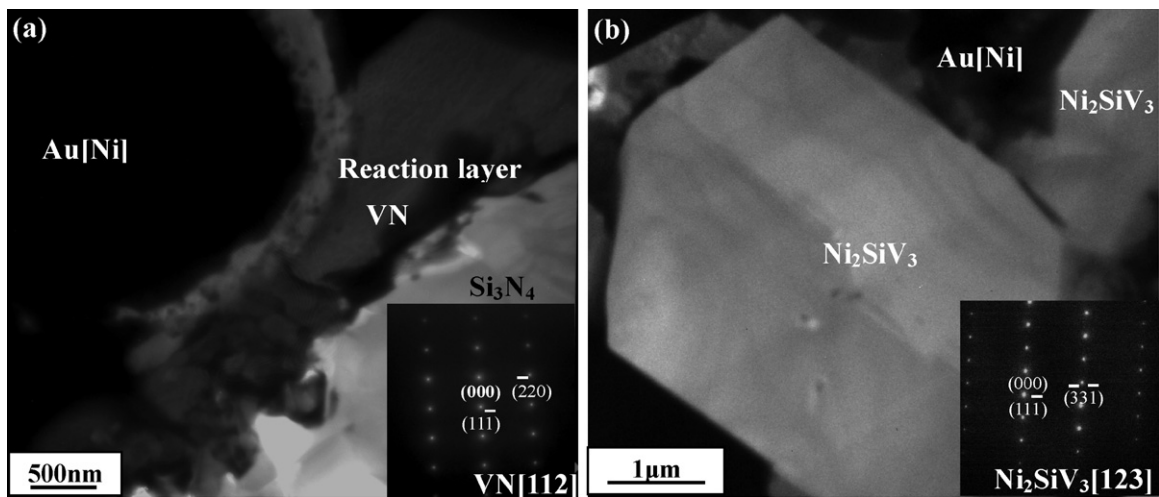


Fig. 4. TEM bright field images and electron diffraction pattern of the reaction layer and polygonal phase in joint brazed by V10 filler alloy: (a) the reaction layer VN, (b) Ni₂SiV₃ phase.

Table 2

Composition at the points A–F shown in Fig. 2(a).

Position	Composition (at.%)							Phase
	Au	Ni	V	Si	N	Al	O	
A	80.4	19.6	–	–	–	–	–	Au[Ni]
B	11.2	88.1	0.2	0.5	–	–	–	Ni[Au]
C	–	–	67.3	–	32.7	–	–	VN
D	0.6	30.7	49.9	16.7	2.1	–	–	Ni ₂ SiV ₃
E	–	72.8	27.2	–	–	–	–	Ni ₃ V
F	–	–	–	–	–	38.6	61.4	Al ₂ O ₃

Fig. 2 shows the microstructure and corresponding element area distribution of the Si₃N₄/Si₃N₄ joint brazed by using V20 filler alloy. The composition of positions A–F is measured by EDS and the results are shown in Table 2. Based on Fig. 2(b) and (c) and EDS analysis results, the matrix alloy labeled as “A” is also Au[Ni] solid solution, and laminar phase “B” is Ni-base solid solution containing 88.1 at.% Ni, 11.2 at.% Au, 0.2 at.% Si and 0.5 at.% V. By comparison of the above Ni[Si, V, Au] solid solution in the joint brazed with V5 or V10 filler alloy, the content of Si and V in laminar solid solution is lower relatively, so it is Au[Ni] solid solution.

As shown in Fig. 2(d), some V was concentrated near the Si₃N₄ ceramic, indicating the VN reaction layer (area C) forming between Si₃N₄ ceramic and the filler. In addition, area “D” was composed of V, Si, and Ni, and the area “E” consisted of V and Ni. According to the composition analysis (Table 2), the phase “D” and “E” is identified as Ni₂SiV₃ phase and Ni₃V intermetallic compound, respectively. Fig. 2(f) shows the distribution of element Al in the joint. It can be seen that most of Al atoms distribute in the ceramic substrate, but a few of Al atoms occur in the area “F”. The composition analysis confirms the phase as Al₂O₃ ceramic particle.

Fig. 1(e) and (f) are the SEM images of the joint brazed with V25 filler alloy, in which the thickness of VN reaction layer reaches 3 μm and a great amount of Ni₂SiV₃ phases are distributed homogeneously in brazing seam. Furthermore, the Ni[Au] solid solution becomes more fine.

In order to identify the phases in the joint and analyze its formation mechanism, TEM analysis was used to testify the reactant phases. Figs. 3 and 4 are the TEM bright field image and electron diffraction pattern of phases in the joint brazed with V10 filler alloy. As shown in Fig. 3, the electron diffraction patterns of phases can testify that the black area is Au[Ni] solid solution with face-centred cubic structure (FCC), the gray phase is FCC structure Ni[Si, V, Au]

solid solution and the bright particles are the Al₂O₃ ceramic with the structure of hexagonal close packed (HCP). The crystal-type and lattice constants of the Al₂O₃ grain is same with that of Al₂O₃ sintering additives in the ceramic substrate. It indicates the Al₂O₃ particles could enter into the molten braze from Si₃N₄ substrate during brazing process.

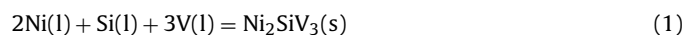
Fig. 4(a) shows morphology of the reaction layer between Si₃N₄ substrate and the filler, which is identified as FCC VN with grain size of 0.5–1 μm. Fig. 4(b) shows a bright field image and electron diffraction pattern of Ni–Si–V ternary phase in the joint. It can be concluded that this phase is Ni₂SiV₃ ternary intermetallic compound with the structure of FCC, which is formed as grains in the brazing seam. This result is consistent with the above EDS analysis in Table 2.

Fig. 5 shows the morphology of the joint brazed with V20 filler alloy and the electron diffraction pattern of reaction layer. The reaction layer between Si₃N₄ ceramic and the filler is also VN with the grain size of 1 μm. The new phase near the reaction layer is identified as Ni₃V with body-centered-tetragonal (BCT) structure by the electron diffraction pattern.

4. Discussion

According to above results and Si–V–N [26], Ni–Si–V [26], Au–Ni [27], etc. phase diagrams, liquid phase appeared between Au and Ni foils when the temperature was increased over 1228 K during brazing. Simultaneously, vanadium was dissolved into the Au–Ni molten metal gradually and aggregated at interface of Si₃N₄ ceramic/molten braze. Si₃N₄ would decompose into Si atoms and N atoms, and N would combine with V to form VN reactant phase, because the free energy of formation for VN (–202.5 kJ/mol) is lower than that for Si₃N₄ (–145.6 kJ/mol) at 1373 K, indicating that VN is more stable than Si₃N₄ [24].

With the interfacial reaction processing continuously, VN grains grew and connected with each other, leading to the formation of the reaction layer. Meanwhile, Si atoms were released from Si₃N₄ and were dissolved gradually into the molten braze, in which Au and Ni atoms were distributed uniformly initial. Due to the strong affinity among Si, V and Ni atoms, Si atoms were gathered around Ni and V atoms in the molten braze, resulting in the formation of enriched Ni radicles. When the content of V is lower relatively in the filler alloy (5 at.%), the reaction layer VN is thinner, so the content of Si released from Si₃N₄ and free V is lower in molten braze. From the Ni–Si–V ternary phase diagram [26], it can be concluded that Ni-base solid solution, including about 8 at.% Si and V, will form during the cooling. When the V content was increased to 10 at.%, the VN grains grew and the thickness of VN reaction layer increased, leading to more Si atoms being released from Si₃N₄. While the atomic ratio among Ni, Si, and V reached 2:1:3, the following chemical reaction would take place at 1373 K:



With reaction (1) proceeding gradually, Si is exhausted, resulting in the reaction termination. When the content of V increases

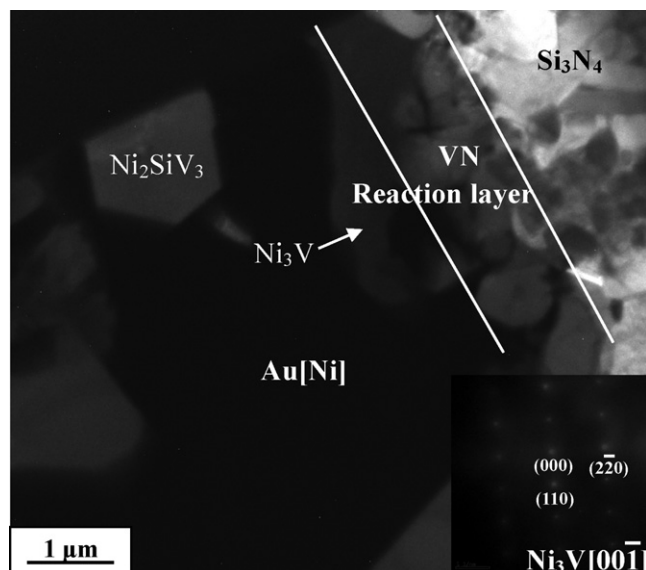


Fig. 5. TEM results of the joint brazed with V20 filler alloy.

further in filler alloy (not less than 15 at.%), due to the excessive addition of V, V element was surplus in molten braze after Si element in the molten braze have been exhausted by reaction (1). According to Ni–V phase diagram, when the atomic ratio of Ni and V reached 3:1, Ni would react with V to form the Ni_3V intermetallic compound at 1318 K during cooling. The reaction is shown as following:



Reaction (2) proceeded until the surplus V in the molten metal was exhausted. Since Si and V elements have been consumed by the above reactions (1) and (2), the center of brazing seam is mainly composed of Au and Ni element during solidification. Finally, Au[Ni] and Ni[Au] solid solution were formed at 1080 K during cooling because the Au and Ni presents a solid state miscibility gap below about 1080 K in Au–Ni phase diagram [27,28].

5. Conclusions

Au–Ni–V filler alloys with different V content were used to braze Si_3N_4 ceramic at 1373 K for 30 min. The high quality joints, which exhibit sound interfacial bonding without any defects between Si_3N_4 and brazing seam, were obtained. The following conclusions were drawn:

- (1) With increasing the V content from 5 to 25 at.%, a VN reaction layer formed between Si_3N_4 ceramic and the filler becomes more continuous and compact. The thickness of reaction layer increases from 0.5 to 3 μm .
- (2) When the joint is brazed using V5 filler alloy, the brazing seam consists of a VN reaction layer, Ni[Si, V, Au] solid solution and the matrix of Au[Ni] solid solution. When the V content increases to 10 at.%, Ni_2SiV_3 phase occurs in the seam, and the Ni[Si, V, Au] precipitate coarsens and VN layer thickens. With increase of V contents to 15 and 20 at.%, laminar Ni[Au] and polygonal Ni_3V precipitates form. With 25 at.% V content in the filler alloy, the Ni_2SiV_3 and Ni_3V precipitates distribute homogenously in the brazing seam.
- (3) The evolution of $\text{Si}_3\text{N}_4/\text{Si}_3\text{N}_4$ joint with the increase of V content reveals three stages of transition as follows: (i) $\text{Si}_3\text{N}_4/\text{VN/Au[Ni]} + \text{Ni[Si, V, Au]}$, (ii) $\text{Si}_3\text{N}_4/\text{VN/Au[Ni]} + \text{Ni[Si, V, Au]} + \text{Ni}_2\text{SiV}_3$, and (iii) $\text{Si}_3\text{N}_4/\text{VN/Au[Ni]} + \text{Ni[Au]} + \text{Ni}_2\text{SiV}_3 + \text{Ni}_3\text{V}$. These microstructure evolutions were attributed to the reaction between Si_3N_4 and

vanadium, which forms VN layer and releases Si into the molten alloy.

- (4) According to the analysis of formation mechanism, the interfacial reactant VN and the polygonal Ni_2SiV_3 phase are formed and grew during the holding time at 1373 K, the Ni_3V phase formed initially during cooling at 1318 K, and the Au-base and Ni-base solid solution were separated below 1080 K.

Acknowledgements

This work was supported by the National Nature Science Foundation of China under the number of 50975064 and 51021002.

References

- [1] C.H. Lee, H.H. Lu, C.A. Wang, P.K. Nayaka, J.L. Huang, J. Alloys Compd. 508 (2010) 540–545.
- [2] J. Zhang, Y.M. He, Y. Sun, C.F. Liu, Ceram. Int. 36 (2010) 1397–1404.
- [3] J.A. Fernie, R.A.L. Drew, K.M. Knowles, Int. Mater. Rev. 54 (2009) 284.
- [4] A.A. Prokopenko, V.S. Zhuravlr, Y.V. Naidich, J. Mater. Sci. Lett. 17 (1998) 2121–2123.
- [5] J.H. Selverian, S. Kang, Weld J. 71 (2002) 25–33.
- [6] M. Gopal, L.D. Jonghe, G. Thomas, Scr. Mater. 36 (1997) 455–460.
- [7] O.M. Akselsen, J. Mater. Sci. 27 (1997) 569–579.
- [8] L. Esposito, A. Bellosi, Scr. Mater. 45 (2001) 759–766.
- [9] R.A. Marks, D.R. Chapman, D.T. Danielson, M. Glaeser, Acta Mater. 48 (2000) 4425–4438.
- [10] L. Esposito, A. Bellosi, J. Mater. Sci. 40 (2005) 4445–4453.
- [11] F. Zhou, J. Mater. Process. Technol. 127 (2002) 293–297.
- [12] X.M. Hou, K.C. Chou, X.J. Hua, H.L. Zhao, J. Alloys Compd. 459 (2008) 123–129.
- [13] C. Iwamoto, S. Tanaka, J. Am. Ceram. Soc. 81 (1998) 363–368.
- [14] A.P. Luz, S. Ribeiro, Ceram. Int. 34 (2008) 305–309.
- [15] J. Zhang, X.M. Zhang, Y. Zhou, M. Naka, A. Svetlana, Mater. Sci. Eng. A 495 (2008) 271.
- [16] Y.M. He, J. Zhang, Y. Sun, C.F. Liu, J. Eur. Ceram. Soc. 30 (2010) 3245–3251.
- [17] M. Paulasto, J.K. Kivilahti, Scr. Metall. 32 (1995) 1209–1214.
- [18] R.E. Loehman, P.G. Kotula, J. Am. Ceram. Soc. 87 (2004) 55–59.
- [19] R.E. Loehman, B.D. Gauntt, F.M. Hosking, P.G. Kotula, S. Rhodes, J.J. Stephens, J. Eur. Ceram. Soc. 23 (2003) 2805–2811.
- [20] H.P. Xiong, W. Dong, B. Chen, Y.S. Kang, A. Kawasaki, H. Okamura, R. Watanabe, Mater. Sci. Eng. A 474 (2008) 376–381.
- [21] M.R. Rijnders, S.D. Peteves, Scr. Metall. 41 (1999) 1137–1146.
- [22] M. Paulasto, C. Cecccone, S.D. Peteves, Scr. Metall. 36 (1997) 1167–1173.
- [23] S.D. Peteves, M. Paulasto, G. Cecccone, V. Stamos, Acta Metall. 46 (1998) 2407–2414.
- [24] J. Zhang, Y. Sun, J. Eur. Ceram. Soc. 30 (2010) 751–757.
- [25] J. Zhang, Y. Sun, C.F. Liu, H.W. Zhang, J. Mater. Sci. 45 (2010) 2188–2193.
- [26] P. Villars, A. Prince, H. Okamoto, Handbook of Ternary Alloy Phase Diagrams, Materials Information Society, ASM International, Materials Park, OH, 1995, pp. 5189–12730.
- [27] M.J. Portmann, R. Erni, H. Heinrich, G. Kosterz, Micron 35 (2004) 695–700.
- [28] R. Voytovych, A. Koltsov, F. Hodaj, N. Eustathopoulos, Acta Mater. 55 (2007) 6316–6321.